Electronic Supporting Information

Ultrahigh Hydrogen Storage Capacity in Novel Porous Aromatic Frameworks†

Xuanjun Wu, [a] Rui Wang, [a] Hongjun Yang, [a] Wenxuan Wang, [a] Weiquan Cai,*[a]

Qingzhong Li [b]

[a]School of Chemistry, Chemical Engineering and Life Sciences, Wuhan University of Technology, Wuhan 430070, P. R. China, and [b]The Laboratory of Theoretical and Computational Chemistry, School of Chemistry and Chemical Engineering, Yantai University, Yantai 264005, P. R. China University, Yantai 264005, P. R. China

The supporting information material includes three sections. Section 1 describes how to construct the molecular models of porous aromatic frameworks (PAFs) with the organic linkers inserted in each C-C bond of diamond framework. The detail structure properties of all PAFs are also listed in this section. Section 2 describes the force field used in this work and the computation details about grand canonical Monte Carlo (GCMC) simulations. Section 3 describes the optimized geometry of PAF-334 and its properties of H_2 adsorption. Section 4 describes the volumetric H_2 uptakes in the four novel PAFs at room temperature. Section 5 lists the references cited in the electronic supporting information part.

S.1. Structure Properties of Porous Aromatic Frameworks

We used density-functional theory (DFT) calculations to predict the structures for the four linkers, DPA, DPB, BPEB and BPBB. Ab initio calculations for optimizations were carried out at the DFT level with B3LYP functional and 6-31++G(2p,2d) basis set using the program Gaussian 09.[1] The optimized geometry of the linkers was listed in Figure S1, which were used to build the molecular models of the four novel PAFs. We adopted the unit cell models of PAF-30X (X=1~4) reported by Ben et al.[2], illustrated in Figure S2. The detail structural properties of all PAF materials are listed in Table S1.

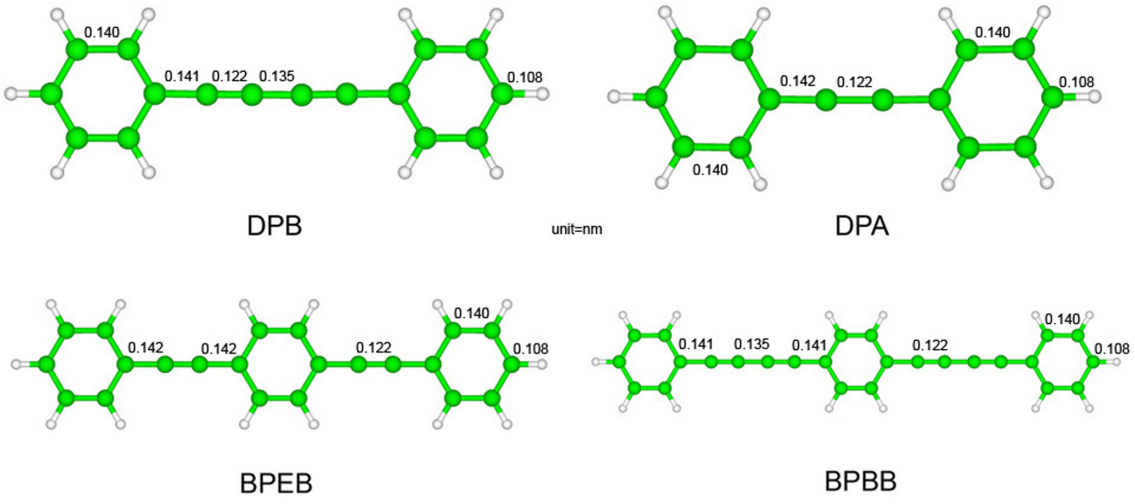

Figure S1. Optimized structures of the four linkers used to build the novel PAFs. White ball, hydrogen atom; green ball, carbon atom.

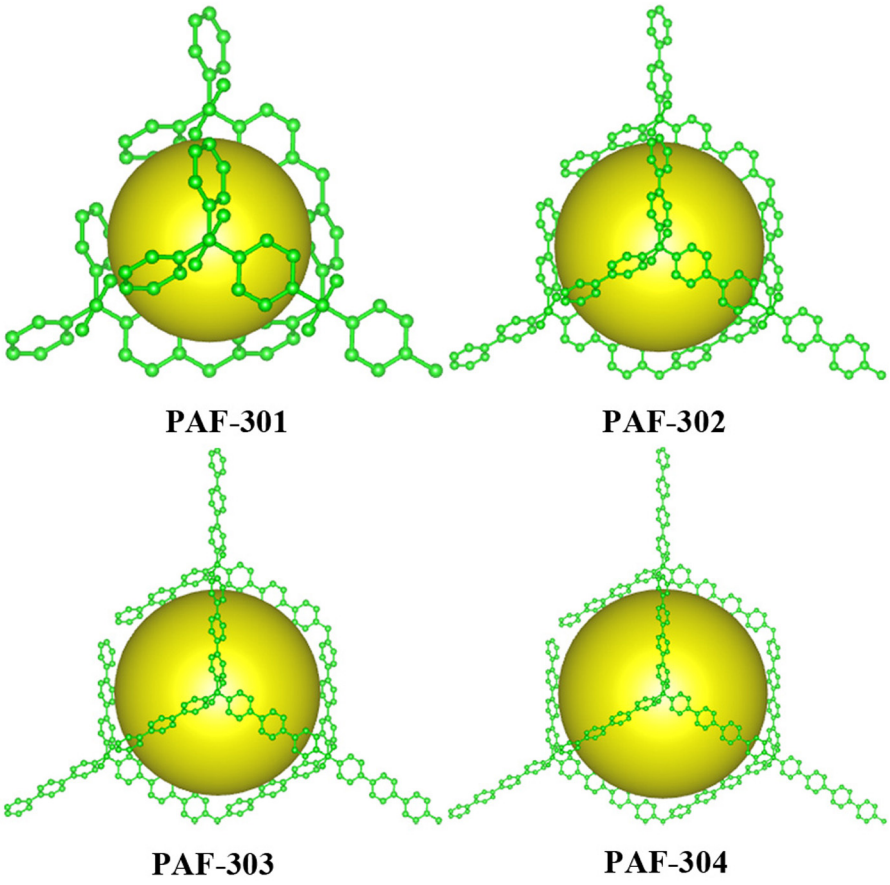

Figure S2. 3D unit cells of the previous PAFs reported by Ben et al.[2] Here the yellow sphere denotes the free pores in different PAFs, and all hydrogen atoms are not shown for clarity.

Table S1. Formula and various properties of PAFs considered in this work.

PAFs	*unit cell formula*	*unit cell type*	*unit cell size* a(nm)	*Density* g cm^{-3}	V_p [a] cm^3 g^{-1}	*SSA* [a] m^2 g^{-1}
PAF-301	$C_{104}H_{64}$	cubic	1.37651	0.8364	0.489	3815.9
PAF-302	$C_{200}H_{128}$	cubic	2.37195	0.3150	2.463	4718.7
PAF-303	$C_{296}H_{192}$	cubic	3.34614	0.1611	5.431	4896.2
PAF-304	$C_{392}H_{256}$	cubic	4.36691	0.0998	9.228	5116.6
PAF-322	$C_{232}H_{128}$	cubic	2.96065	0.1866	4.744	5244.8
PAF-324	$C_{264}H_{128}$	cubic	3.54955	0.1225	7.556	5371.8
PAF-332	$C_{360}H_{192}$	cubic	4.54490	0.0799	11.898	5686.9
PAF-334	$C_{424}H_{192}$	cubic	5.72270	0.0468	20.749	5782.0
PAF-322OP	$C_{232}H_{128}$	cubic	2.96065	0.1866	4.746	5218.0
PAF-324OP	$C_{264}H_{128}$	cubic	3.54955	0.1225	7.558	5361.0
PAF-332OP	$C_{360}H_{192}$	cubic	4.54490	0.0799	11.903	5660.9
PAF-334OP	$C_{424}H_{192}$	cubic	5.72270	0.0468	20.751	5762.8

[a] Calculated by Düren's method from Ref.3, using N_2 as probe molecule of 3.681Å diameter. V_p denotes free pore volume of cell. *SSA* denotes specific surface area of cell.

S.2. Force Field and GCMC Computation Methods

The adsorption isotherms of H_2 molecules on PAFs were predicted using grand canonical Monte Carlo (GCMC) simulations, based on the force field derived from the first-principles calculations. All GCMC simulations were performed using our modified Multipurpose Simulation Code (MuSiC-4.0), which is originally developed by Snurr group.[4] We adopted the following Morse potential function to describe the nonbonded interactions between H_2 and PAFs.

$$U_{ij}(r_{ij}) = D\left\{\exp\left[\alpha(1-\frac{r_{ij}}{r_e})\right] - 2\cdot\exp\left[\frac{\alpha}{2}(1-\frac{r_{ij}}{r_e})\right]\right\} \qquad (1)$$

Where D, r_e and α is the well depth, the equilibrium bond distance, and the force constant, respectively. A two-atom model was used to describe the hydrogen molecule with a characteristic distance H-H of 0.074nm.[5] The force field parameters for nonbonded interaction between H_2 and PAFs were directly referenced from previous literatures (see Table S2).[6, 7]

Table S2. van der Waals force field parameters for nonbond interactions between H_2 and PAFs.

Atom types	Morse potential parameters		
	D(kcal mol^{-1})	r_e (nm)	α
H_A---H_A[a]	0.0182	0.35698	10.7094
H_---H_A[a]	0.0124	0.32010	12.0027
C_R---H_A[a]	0.0892	0.32400	11.6000
C_3---H_A[a]	0.0620	0.32400	11.0062
C_1---H_A[b]	0.1024	0.31793	10.3975

[a]From Ref.6 ,[b]From Ref.7. Here H_A denotes H atom in a H_2 molecule. H_ denotes H atom bonded to the hydrocarbon rings. C_R, C_3 and C_1 denote sp^2 aromatic, sp^3 and sp^1 C atoms, respectively.

Chemical potentials of gas sorbates at different temperature and pressure were converted to fugacity with the Peng-Robinson equation of state (PREOS).[8] Absolute adsorbed amounts (N_{abs}) obtained by GCMC simulations are converted to excess adsorbed amounts (N_{exc}), using the following equation

$$N_{exc} = N_{abs} - \rho_{bulk} \cdot V_{free} \qquad (2)$$

Where N_{abs} is the amount of absolute adsorbed molecules, V_{free} represents the pore volume of adsorbent, and ρ_{bulk} is the density of the sorbate calculated using PREOS at a

given temperature and pressure.[9] The numbers of unit cells of PAFs adopted in this simulation were 2×2×2 or 1×1×1 if their unit cells are too big, and periodic boundary conditions were applied in all three dimensions to eliminate boundary effects. The PAFs were treated as rigid with frozen atoms during simulation.[10] Cutoff radius of nonbonded interactions is 1.2 nm. A total of 10^7 steps were used; the first half of these moves was used for equilibration, and the remaining steps were used for calculating the ensemble averages. Four types of moves (translation, random insertion, rotation and deletion) were used. Every possible move was given equal probability.

S.3. The optimized geometry of PAF-334 and its properties of H_2 adsorption

The atomic coordinates of the four novel PAFs were optimized with LAMMPS code[11] and PCFF force field.[12] The partial charges of all types of atoms in these PAFs were directly taken from the PCFF force field. Cutoff radius of electrostatic interactions is 1.2 nm, and long-range electrostatic interactions are treated via the Ewald method. Cutoff radius of LJ interactions is also 1.2 nm, and periodic boundary conditions were applied in all three dimensions. To obtain the best structures, no space group symmetry constraints were imposed on the frameworks and all the bond lengths, angles, and cell parameters were well optimized. The geometries were optimized until the remaining atomic forces were less than 0.0001 kcal (mol^{-1} $Å^{-1}$) on each atom and the energy convergence criterion was chosen as 1.0×10^{-5} kcal mol^{-1} between two steps. The structural properties of optimized PAFs(termed as PAF-322OP, PAF-324OP, PAF-332OP and PAF-334OP, respectively) were also calculated by the aforementioned method. The results are also listed in Table S1, indicating that there is little difference of the major structural parameters between optimized and original PAFs. For example, free

pore volume (V_p) and specific surface area (SSA) of PAF-334OP are 20.751 $cm^3\ g^{-1}$ and 5762.8 $m^2\ g^{-1}$, respectively, while the ones of PAF-334 are 20.749 $cm^3\ g^{-1}$ and 5782.0 $m^2\ g^{-1}$, respectively. The total H_2 uptakes in optimized PAFs at different temperatures were also calculated by GCMC simulations and compared with the ones of original PAFs (see Figures S3-S6). The results show that the total H_2 uptakes in each optimized material are all in good agreement with the ones in its original structure at different temperatures, indicating that the simulated results of H_2 uptakes in the four original frameworks are credible in spite of skipping the crystal structure optimization of PAFs.

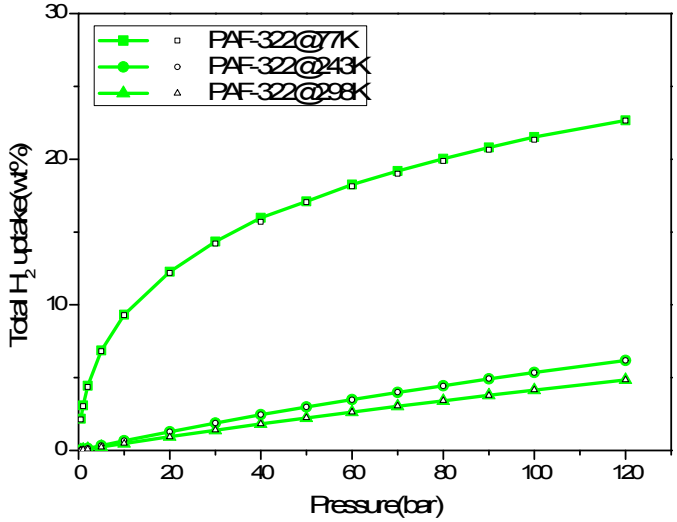

Figure S3. Simulated adsorption isotherms of H_2 in original PAF-322(open symbols) and optimized PAF-322(filled symbols) at different temperatures.

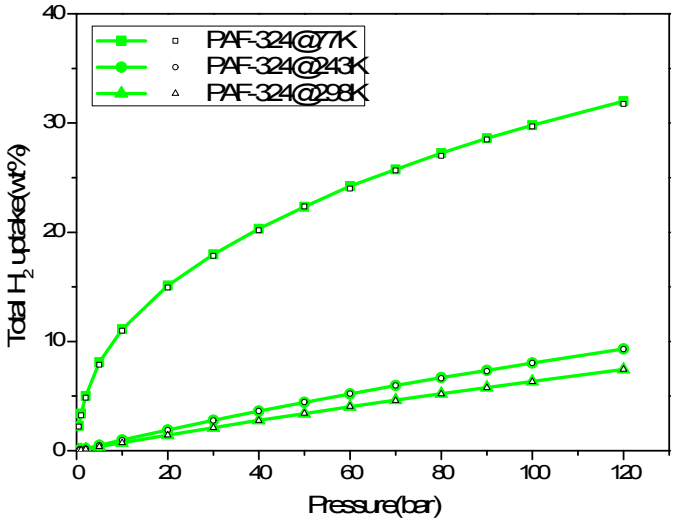

Figure S4. Simulated adsorption isotherms of H_2 in original PAF-324(open symbols) and optimized PAF-324(filled symbols) at different temperatures.

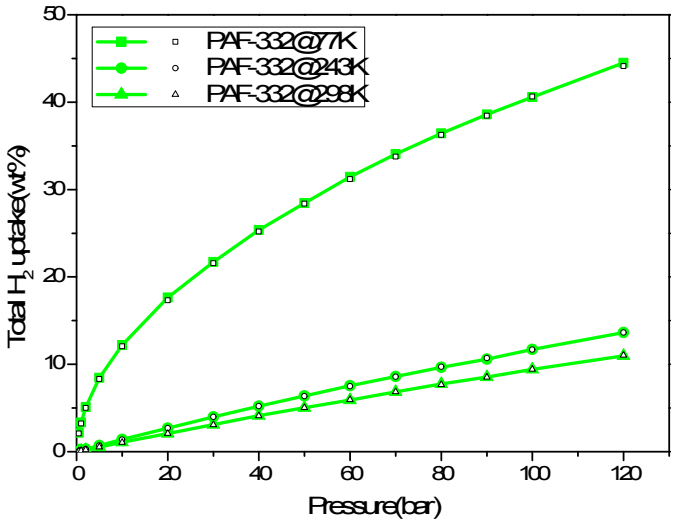

Figure S5. Simulated adsorption isotherms of H_2 in original PAF-332(open symbols) and optimized PAF-332(filled symbols) at different temperatures.

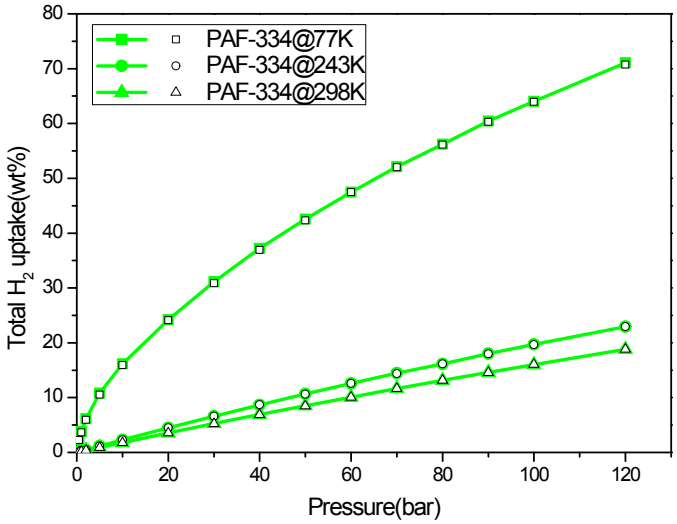

Figure S6. Simulated adsorption isotherms of H_2 in original PAF-334(open symbols) and optimized PAF-334(filled symbols) at different temperatures.

S.4. Volumetric H_2 uptakes in the novel PAFs at room temperature

Figures S7-S8 show the total volumetric adsorption isotherms of H_2 in the four novel PAFs at 243K and 298K, respectively.

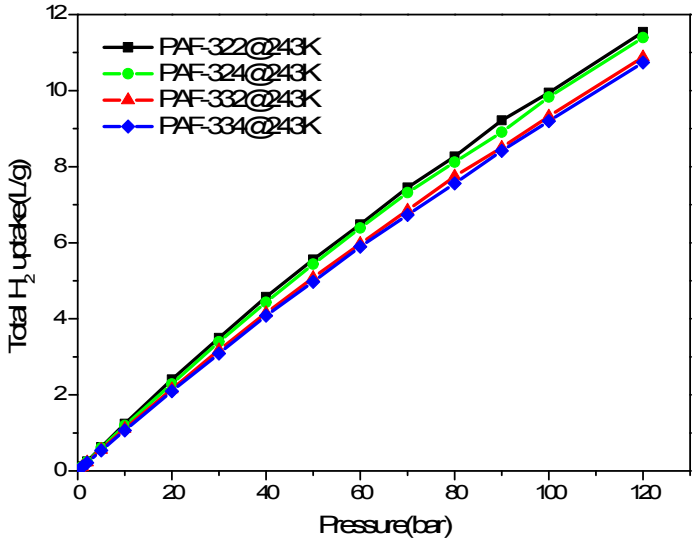

Figure S7. Simulated total volumetric adsorption isotherms of H_2 in the four novel PAFs at 243K.

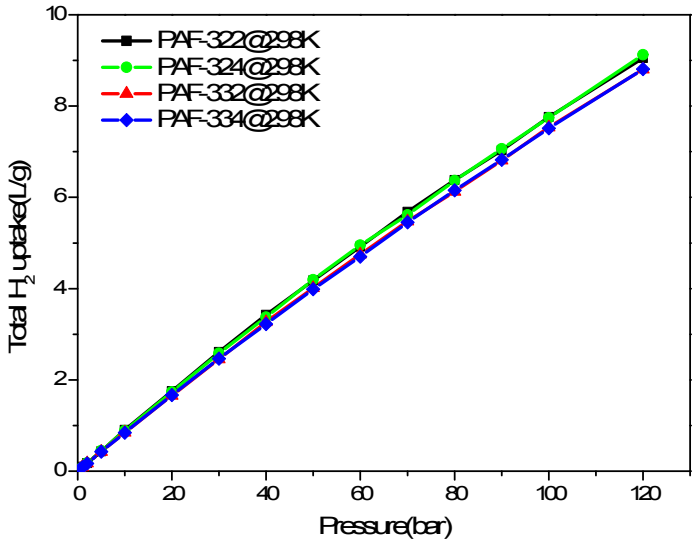

Figure S8. Simulated total volumetric adsorption isotherms of H_2 in the four novel PAFs at 298K.

S.5. References

1. G. W. T. M. J. Frisch, H. B. Schlegel, G. E., M. A. R. Scuseria, J. R. Cheeseman, G. Scalmani, V. Barone, B. Mennucci,, H. N. G. A. Petersson, M. Caricato, X. Li, H. P. Hratchian, A. F., J. B. Izmaylov, G. Zheng, J. L. Sonnenberg, M. Hada, M. Ehara, K. Toyota,, J. H. R. Fukuda, M. Ishida, T. Nakajima, Y. Honda, O. Kitao, H. Nakai,, J. A. M. T. Vreven, Jr., J. E. Peralta, F. Ogliaro, M. Bearpark, J., E. B. J. Heyd, K. N. Kudin, V. N. Staroverov, R. Kobayashi, J. Normand,, A. R. K. Raghavachari, J. C. Burant, S. S. Iyengar, J. Tomasi, M. Cossi,, J. M. M. N. Rega, M. Klene, J. E. Knox, J. B. Cross, V. Bakken, C. Adamo,, R. G. J. Jaramillo, R. E. Stratmann, O. Yazyev, A. J. Austin, R. Cammi,, J. W. O. C. Pomelli, R. L. Martin, K. Morokuma, V. G. Zakrzewski, G., P. S. A. Voth, J. J. Dannenberg, S. Dapprich, A. D. Daniels, Ö. Farkas, and J. V. O. J. B. Foresman, J. Cioslowski, and D. J. Fox, Gaussian, Inc.,Wallingford CT, 2009.
2. T. Ben, H. Ren, S. Ma, D. Cao, J. Lan, X. Jing, W. Wang, J. Xu, F. Deng, J. M. Simmons, S. Qiu and G. Zhu, *Angew. Chem. Int. Ed.*, 2009, **48**, 9457-9460.
3. T. Düren, F. Millange, G. Ferey, K. S. Walton and R. Q. Snurr, *J. Phys. Chem. C*, 2007, **111**, 15350-15356.
4. A. Gupta, S. Chempath, M. J. Sanborn, L. A. Clark and R. Q. Snurr, *Mol. Simul.* , 2003, **29**, 29-46.
5. Z. Yang and D. Cao, *J. Phys. Chem. C*, 2012, **116**, 12591-12598.
6. J. Lan, D. Cao, W. Wang, T. Ben and G. Zhu, *J. Phys. Chem. Lett.*, 2010, **1**, 978-981.
7. A. Li, R.-F. Lu, Y. Wang, X. Wang, K.-L. Han and W.-Q. Deng, *Angew. Chem. Int. Ed.*, 2010, **49**, 3330-3333.
8. D.-Y. Peng and D. B. Robinson, *Ind. Eng. Chem. Fund.*, 1976, **15**, 59-64.
9. X. Wu, J. Huang, W. Cai and M. Jaroniec, *RSC Adv*, 2014, **4**, 16503-16511.
10. X. Wu, P. Zhao, J. Fang, J. Wang, B. Liu and W. Cai, *Acta Phys. -Chim. Sin.*, 2014, **30**, 2043-2054.
11. S. Plimpton, *J. Comp. Phys.*, 1995, **117**, 1-19.
12. H. Sun, S. J. Mumby, J. R. Maple and A. T. Hagler, *J.Am.Chem.Soc.*, 1994, **116**, 2978-2987.